Journal of Materials Science Research and Reviews

8(4): 164-171, 2021; Article no.JMSRR.77178

Novel White Light Emitting ($Ca_2MgSi_2O_7:Dy^{3+}$) Phosphor

Shashank Sharma[1*], Sanjay Kumar Dubey[1], A. K. Diwakar[1] and Sanjay Pandey[2]

[1]Department of Physics, Kalinga University, Naya Raipur, C.G., India.
[2]Department of Physics, Bhilai Institute of Technology, Raipur, C.G., India.

Authors' contributions

This work was carried out in collaboration among all authors. All authors read and approved the final manuscript.

Article Information

Editor(s):
(1) Prof. Yong X. Gan, California State Polytechnic University, USA.
Reviewers:
(1) Cliff Orori Mosiori, Technical University of Mombasa, Kenya.
(2) Zuoxiang Zeng, East China University of Science and Technology, China.
Complete Peer review History: https://www.sdiarticle4.com/review-history/77178

Original Research Article

Received 07 September 2021
Accepted 15 November 2021
Published 19 November 2021

ABSTRACT

$Ca_2MgSi_2O_7:Dy^{3+}$ (CMSD) white light emitting phosphor was synthesized by combustion route process. In order to find out the phase purity and crystal structure, characterization of the prepared powder samples was done by X-ray diffraction (XRD) technique. The results of the XRD study obtained for CMSD phosphor revealed its tetragonal crystal structure with a space group $P\bar{4}2_1m$. XRD pattern well matched with the help of standard JCPDS Pdf file No. 17-1149. The average crystallite size was calculated as 28.71nm and strain as 0.27. The actual structure formation and identifying functional group was confirmed by Fourier transform infrared spectroscopy. The FTIR results confirms that the synthesized phosphor has a better phase formation and this phosphor contains chemical bonds and Functional group such as (Mg-O), (Si-O), (O-Si-O) and (CO_3^{2-}), (O-H) as well as (SiO_4). The prepared phosphor was excited at 357 nm and their corresponding emission spectra were recorded at blue (476 nm), yellow (578 nm) and red (615 nm) spectral line peaking due to the $^4F_{9/2} \rightarrow {}^6H_{15/2}$, $^4F_{9/2} \rightarrow {}^6H_{13/2}$, $^4F_{9/2} \rightarrow {}^6H_{11/2}$, transitions of Dy^{3+} ions respectively. In this paper, structural characterizations such as XRD, FTIR, and optical properties like photoluminescence spectra of this phosphor are also reported.

**Corresponding author: Email: dr.shashankeinstein@rediffmail.com;*

Keywords: X-ray diffraction (XRD); Photoluminescence (PL); $Ca_2MgSi_2O_7:Dy^{3+}$ (CMSD); Tetragonal.

ABREVIATIONS

WLEDs	*: White Light Emitting diodes*
RE	*: Rare Earths*
FTIR	*: Fourier Transform Infra-Red Spectroscopy*
XRD	*: X-Ray Diffraction*
KBr	*: Potassium Bromide*
LEPs	*: Light emitting phosphors*
S	*: Solid*
aq	*: Liquid*
g	*: Gas*
$Ca_2MgSi_2O_7:Dy^{3+}$	*: CMSD*

1. INTRODUCTION

Material scientists and researchers have found that the WLEDs as a solid-state light source have emerged in the form of major attraction [1,2]. In addition, it has been also observed that the rare-earth doped inorganic luminescent phosphors are quite applicable in most devices for the generation of artificial light [3]. The combustion method has proven its usefulness as an easy route for the synthesis of a variety of homogenous phosphors, including silicates and aluminates, which is very suitable for the phosphor preparation at low temperature and much shorter time period as compared to expensive high temperature furnace [4-6]. Thus, this method has been successfully employed for the synthesis of WLED phosphors. This method confers control over the morphology and particle size of the synthesized phosphors [7]. Research on various RE doped phosphors in recent years has led to very unprecedented results. They have gained widespread interest due to their inherent thermally stability, larger band gap, higher elemental stability, low consumption, structural diversity and environmental personality properties [8-10]. $Sr_2MgSi_2O_7:Eu^{2+}$, Dy^{3+} is the best stable luminescent silicate phosphor. But long afterglow characteristics have also been discovered in many silicate materials. Later, fluorescence and after-glow characteristics in $Ca_2MgSi_2O_7:Eu^{2+}$, Tb^{3+} has been observed similar to $Sr_2MgSi_2O_7:Eu^{2+}$, Dy^{3+} phosphor, to be maximum at 515/535nm wavelength in greenish spectrum region [11]. The silicate phosphors displayed some benefits over the already evolved aluminates long persistent phosphors over the varied luminescence color from blue to yellow [12]. Jiang (2004) et al. also discussed that in di calcium magnesium di silicate crystal structure, dysprosium (Dy^{3+}) is expected to occupy the calcium cation (Ca^{2+}) site preferably because the ionic radius of Dysprosium (Dy^{3+}) 0.97 Å is very nearby to that of di valent calcium cation (Ca^{2+}) 1.12 Å but di valent magnesium cation (Mg^{2+}) 0.58 Å and tetra valent silicon cation (Si^{4+}) 0.26 Å are too small for dysprosium [Dy^{3+}] occupation [13]. Dysprosium (Dy^{3+}) rare earth ion plays a chief role in the generation of various types of LEPs [14]. Raut et al. (2011) investigated that the $Ca_2MgSi_2O_7$: Dy^{3+} phosphor displayed emission peaks at 462 nm (blue) and 576 nm (yellow) wavelengths in the visible region, when stimulated at 384 nm wavelength. [15]. Bhatkar et al. also reported that for tissue engineering applications, silicate based bio-ceramics are promising candidates as biomaterials [7].

In this paper, white light emitting phosphor $Ca_2MgSi_2O_7:Dy^{3+}$ (4mol %) were successfully synthesized via combustion route and its structural properties such as XRD (X-Ray Diffraction) as well as functional group identification using FTIR (Fourier Transform Infra-Red Spectroscopy) and optical properties such as photoluminescence (PL) spectra have also be discussed.

2. EXPERIMENTAL DETAILS

2.1 Sample Preparation

We have employed in our experiment the powder sample with the general formula $Ca_{2-x}MgSi_2O_7$: Dy_x^{3+} (4mol %) phosphor was prepared via the combustion synthesis method. All initial reagents with (99.99%) purity, Ca $(NO_3)_2$ (AR), Mg $(NO_3)_2$ (AR), SiO_2*H_2O (AR), NH_2CONH_2 (Urea) (AR), H_3BO_3 (boric acid) (AR) and rare earth nitrate Dy $(NO_3)_3$ (AR) were utilized as starting materials. Very little quantities were used urea (NH_2CONH_2) as a combustion fuel and H_3BO_3 (boric acid) (AR) as a flux. It was very mandatory in our experiment that the entire precursor reagents with suitable molar ratio were dissolved in a very little amount of acetone (CH_3COCH_3) homogeneously to get a clear solution. The weighed quantities of each nitrates, flux and fuel were mixed into agate mortar and pestle (diameter-5'') in clock wise direction for 5 min to convert into a thick paste. After the solution is transferred into the cylindrical silica crucible with comparatively larger volume as well as it is placed into a muffle furnace already maintained at 650^oC temperature. The entire combustion

process was completed in about 5 min. Within a few minutes, the mixture solution undergoes thermal dehydration with liberation of gaseous products, to growth silicates and ignites to produce a self-propagating flame Fig. 1(a). After next few seconds, and as it is over, crucible is taken out of furnace and kept in open to allow cooling. Upon cooling Fig. 1(b), we acquire fluffy form of phosphor, which is then grinded with the help of agate mortar pestle (diameter-5'') to obtain material in the powder form. The final product obtained was post-annealed at 950°C for 1 h under an air atmosphere. Applying additional grinded into a fine powder. The resulting sample was restored in airtight bottle for characterization studies.

The chemical reaction of this process is given as follows:

$Ca\ (NO_3)_2(s) + Mg\ (NO_3)_2(s) + SiO_2{*}H_2O(s) + NH_2CONH_2(s) + Dy\ (NO_3)_3(s) \rightarrow Ca_2MgSi_2O_7:Dy^{3+}(s) + H_2O\ (g)\ (\uparrow) + CO_2\ (g)\ (\uparrow) + N_2\ (g)\ (\uparrow)$ (1)

We have generally agreed that the fuel and oxidizers are needed for any combustion synthesis process. Metal nitrates are also employed as oxidizers and urea is also applied as a fuel. On the basis of propellant chemistry, the stoichiometric compositions of all metal nitrates and fuel are calculated. Thus, the heat of combustion is maximum for Oxidizer/Fuel ratio is equal to 1 [16].

2.2 Measuring Instruments

The raw reagents are weighed with the help of Shimadzu ATX 224 single pan analytical balance. XRD of the crystalline structure, size and phase composition of the synthesized phosphor were noted with the help of Bruker D8 advance X-ray diffractometer with Cu-K_α radiation having wavelength (λ = 1.5406 Å, at 40 kV, 40 mA), respectively. Actual formation of this phosphor was obtained through FTIR. An FTIR spectrum was recorded with the help of Bruker Alpha Fourier transform Infra-red Spectroscopy. For investigating the functional groups (4000 to 1400 cm^{-1}) as well as the finger print area (1400 to 400 cm^{-1}) of synthesized phosphor through mixing the sample with analytical grade potassium bromide (KBr) with pallet preparation. In photoluminescence spectra (PL), emission spectra were recorded by a spectro-fluorophotometer (SHIMADZU, RF-5301 PC) using a xenon lamp of power 150 watt as excitation source. All experiments were performed in identical conditions and it was observed that the results were reproducible. All measurements recorded at the room temperature.

3. RESULTS AND DISCUSSION

3.1 X-ray Diffraction (XRD)

XRD patterns of $Ca_2MgSi_2O_7:Dy^{3+}$ phosphor synthesized by combustion route method is shown in Fig. 2. It is recorded in the range (10^o\2θ\$80^o$). All the peaks show well agreement with the JCPDS No. 17-1149 [17]. The phase formation of the prepared phosphors was also confirmed by XRD characterization. The standard $Ca_2MgSi_2O_7$ structure, cell volume and lattice parameters are observed from data base code AMCSD 0008032 [18]. It is also observed that the influence of doping doesn't affect the phase structure of the phosphor. On this basis, we can say that the Dy^{3+} ion are expected to occupy the Ca^{2+} sites in the $Ca_2MgSi_2O_7$ host. This structure is a member of the melilite group and produces a layered compound.

Fig. 1(a). Heating process of CMSD phosphor

Fig. 1(b). Prepared CMSD Foam

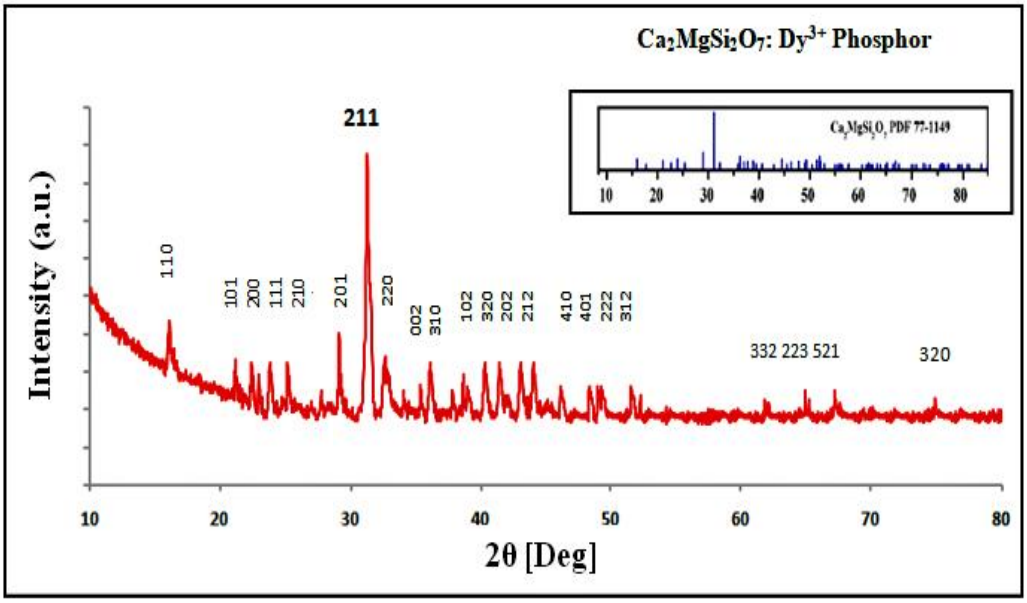

Fig. 2. XRD pattern of $Ca_2MgSi_2O_7$:Dy^{3+} phosphor

3.2 Debay Scherrer Formula

An estimation of average crystalline size for the $Ca_2MgSi_2O_7$: Dy^{3+} phosphor is done using Scherrer's formula; its mathematical representation as follows:

$$D = K\lambda/\beta Cos\theta \quad (2)$$

Where D is the crystalline size, K=0.94 (Scherrer constant), λ indicates the wavelength of incident X-ray (for Cu Kα radiation, λ = 1.5406 Å), β is the FWHM (Full width half maximum) of the peaks and θ is the corresponding Braggs diffraction angle [19-20].

3.3 Strain Determination by Uniform Deformation Model (UDM)

The strain induced broadening in the powder material was calculated via the following formula given as below:

$$\varepsilon = \beta/4tan\theta \quad (3)$$

Table 1 shown all parameters of the CMSD phosphor. In this sequence, the sintered CMSD phosphor was confirmed with a tetragonal crystal structure with a space group $P\bar{4}2_1m$. Whose lattice parameters are a=b= 7.8071 Å and c=4.9821 Å as well as $\alpha=\beta=\gamma=90^o$ and cell volume is 303.663 $(Å)^3$. The crystallize size of the prepared phosphor, according to the dominant peak (211), yielded 28.71nm at 31.24 [2θ deg]. In addition, The crystal plane spacing (d) 2.8630Å and strain 0.27 were calculated.

3.4 FTIR Spectra

3.4.1 Potassium Bromide (KBr) Pallet Preparation

The Potassium Bromide (KBr) pallet is prepared including with CMSD phosphor, before recording the FTIR spectra of a synthesized sample. It is very essential to mix the sintered sample with KBr (IR Grade) powder and grind it. After applying with hydraulic pressure to form a thin pallet. It is very important to be noted that the KBr powder and CMSD sample should be taken in very little amounts. So that, the pallet can becomes thinner. In this way, FTIR spectra and reading are obtained very clearly.

3.4.2 Functional group Discussion

Fig. 3(a) demonstrates the FTIR spectrum of dysprosium doped di calcium magnesium di silicate phosphor. FTIR spectra were carried out in the range of (4000-400 cm^{-1}). This spectra revealed that the actual formation and evidence of functional group in phosphor. As the dysprosium [Dy^{3+}] ions enters in $Ca_2MgSi_2O_7$ host lattice, most of the FTIR peaks become sharp. This is mainly because of exhibiting a preferable crystal perfection of tri-valent dysprosium [Dy^{3+}] ions. The large band at 981.83

cm^{-1} and 942.27 cm^{-1} for Si-O-Si asymmetric stretch was examined to be more prominent because of dysprosium [Dy^{3+}] doping and there was shift of bands at 845.65 cm^{-1},745.43 cm^{-1} are allocated to the vibration in the calcium [Ca^{2+}] ions. We see that the O-Si-O bands at 686.95 cm^{-1} and 646.30 cm^{-1} can be allocated because of the existence of silicate [SiO_4] functional group. At 1910.35 cm^{-1}, band centered can be merited because of the existence of little amount of calcite. At 493.83 cm^{-1}, band centered because of the Mg-O banding. The asymmetry stretching can be allocated because of the evidence of carbonate [CO_3^{2-}] functional group, spectrum band situated at 1910.37 cm^{-1} and band at 1636.23 cm^{-1} was allocated because of the vibration in magnesium [Mg^{2+}] ions. The evidence of hydroxyl [O-H] functional group because of the stretching vibration, band was centered at 3436.20 cm^{-1} [21-27].

3.5 Photoluminescence Spectra

The excitation and emission spectra of dysprosium rare earth doped di calcium magnesium di silicate CMSD ($Ca_2MgSi_2O_7$: Dy^{3+}) phosphor are shown in Fig. 3(b) & 3(c). Emission at wavelength 476nm ascribed to transition ($^4F_{9/2} \rightarrow {}^6H_{13/2}$), the excitation spectra showed in Fig. 3(b). We observed that a series of spectral lines are acquired in the range between (340 nm – 470 nm), excitation with the strongest peak at 357 nm transition ($^6H_{15/2} \rightarrow {}^4I_{13/2}$) because of the 4f-4f transition of the dysprosium [Dy^{3+}] ions. Simultaneously, there are some other spectral lines allocated wavelengths at 367nm, 386nm, 429nm and 457nm, respectively. Which are fixed to the transition from the ground state (lower energy) to excited states (high energy) in the $4f^9$ configuration of dysprosium [Dy^{3+}].

Table 1. According to prominent peak (211) of the XRD pattern of CMSD phosphor and the calculation value of parameters

No.	Parameters	$Ca_2MgSi_2O_7:Dy^{3+}$ Phosphor
1.	**Crystal Structure**	Tetragonal
2.	**Space Group**	$P\bar{4}2_1m$
3.	**Lattice Parameters**	a=b=7.8071Å, α=β=γ=90° c=4.9821Å
4.	**Crystallize Size D(nm)**	28.71nm
5.	**2 Theta (Deg)**	31.24nm
6.	**Cell Volume**	303.663 $(Å)^3$
8.	**Crystal Plane Spacing d(Å)**	2.8630(Å)
9.	**Strain**	0.27

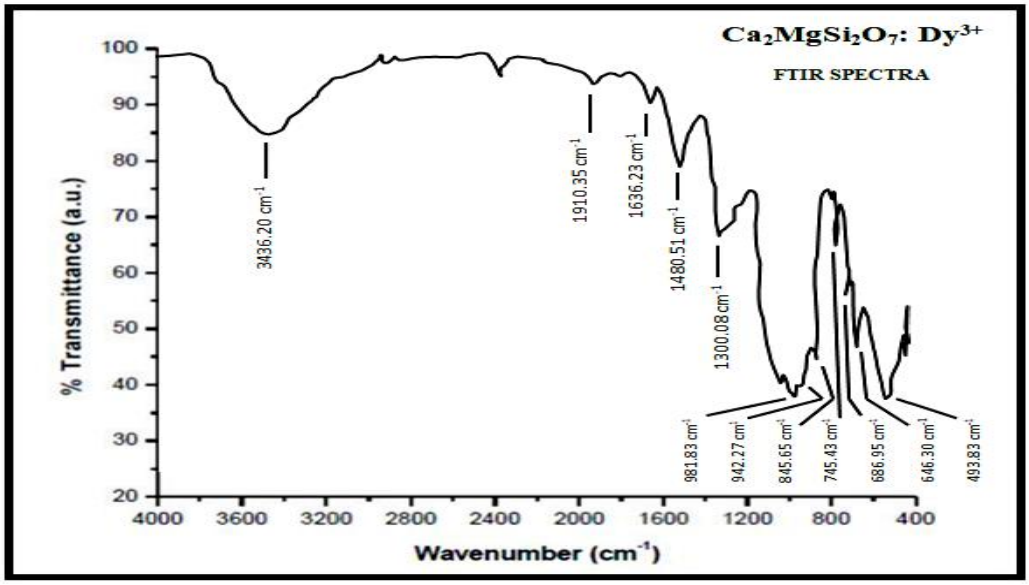

Fig. 3(a). FTIR Spectra of CMSD phosphor

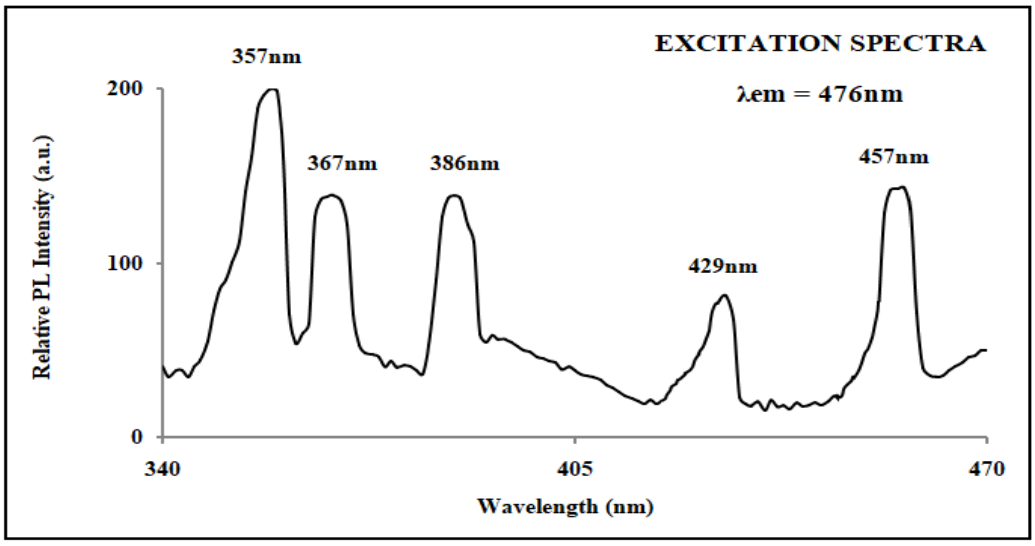

Fig. 3(b) Excitation spectra (λem = 476nm) of the $Ca_2MgSi_2O_7:Dy^{3+}$ phosphor

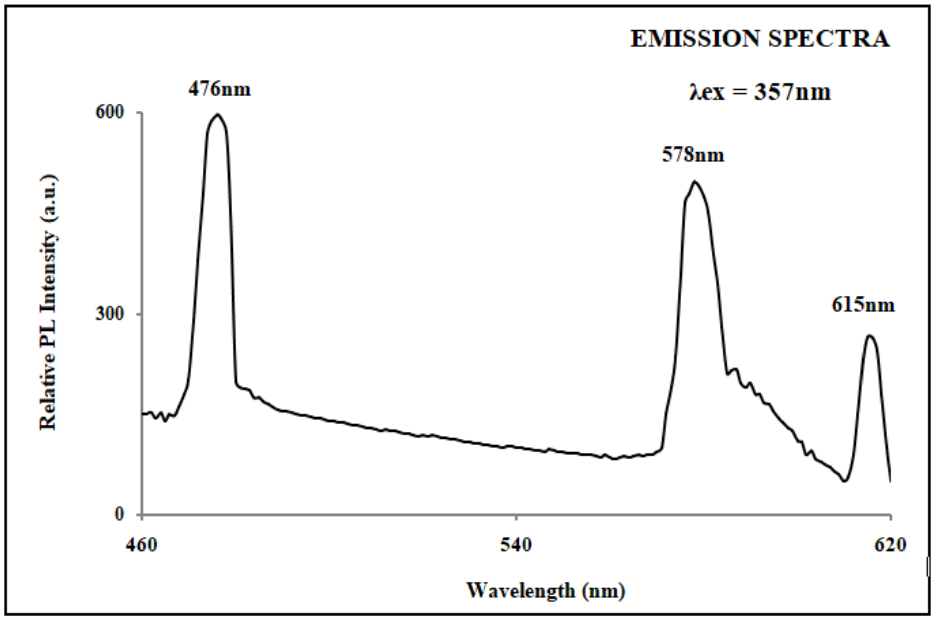

Fig. 3(c). Emission spectra (λex = 357nm) of the $Ca_2MgSi_2O_7:Dy^{3+}$ phosphor

Fig. 3(c) is showing the PL (photoluminescence) emission spectra of CMSD ($Ca_2MgSi_2O_7$: Dy^{3+}) phosphor. At 357 nm wavelength, they were recorded under excitation spectrum in the range between (460 to 620nm). The emission spectra exhibited intense spectral lines situated at 476nm ($^4F_{9/2}\rightarrow{}^6H_{15/2}$), 578nm ($^4F_{9/2}\rightarrow{}^6H_{13/2}$) and 615 nm ($^4F_{9/2}\rightarrow{}^6H_{11/2}$) because of the intra-configurational 4f–4f transitions of dysprosium [Dy^{3+}] ion. The yellow ($^4F_{9/2}\rightarrow{}^6H_{13/2}$) emission connected to the forced electric dipole transition type is permitted only at low symmetry, in which there is no inversion centre. Synchronously, its intensity is strongly affected by the crystal-field surrounding. The blue band ($^4F_{9/2}\rightarrow{}^6H_{15/2}$) is acquired because of the magnetic dipole transition (476 nm). The red band ($^4F_{9/2}\rightarrow{}^6H_{11/2}$) acquired at 615 nm in emission spectrum corresponds to the dysprosium [Dy^{3+}] ion [28-30].

We have suggested that the main reason to come whiteness from the mixture of dysprosium

[Dy^{3+}] ions emission in blue (476nm) and in yellow (578nm) regions. It is reported that the yellow and blue ratio, also known as the asymmetry ratio of dysprosium [Dy^{3+}] ion, which varies with the host lattices. With an increasing calcinating temperature, the yellow and blue ratio also goes high because of the variation of the local site symmetry around tri-valent dysprosium [Dy^{3+}] ion [31,32].

4. CONCLUSION

In summary, $Ca_2MgSi_2O_7$:Dy^{3+} (4mol %) phosphor were successfully sintered via combustion route process. The XRD spectra displayed that the standard patterns of acquired phosphor were well matched with the help of JCPDS Pdf file No. 77-1149 and lattice parameters were also observed from data base code AMCSD 0008032. The XRD result revealed its tetragonal crystal structure with a space group $P\bar{4}2_1m$. In addition, the average crystallite size was calculated as 28.71nm and strain as 0.27. The FTIR results confirms that the synthesized phosphor has a good phase formation and this phosphor contains chemical bonds and Functional group such as (Mg-O), (Si-O), (O-Si-O), (CO_3^{2-}) and (O-H) as well as ([SiO_4). The CMSD phosphors showed that the higher PL emission intensity allocated at 476 nm (blue), 578nm (yellow) and 615nm (red). The grain size was obtained in nano crystal with superior homogeneity. These peaks were attributed to electronic transition blue ($^4F_{9/2} \rightarrow {}^6H_{15/2}$), yellow ($^4F_{9/2} \rightarrow {}^6H_{13/2}$) and red ($^4F_{9/2} \rightarrow {}^6H_{11/2}$) of dysprosium [$Dy^{3+}$] respectively. The optimum intensity was acquired in 4mol % doping concentration of dysprosium [Dy^{3+}]. These results indicate that synthesized phosphor may be better promising candidate phosphors in the field of solid state lighting and white light long lasting phosphor as well as Drug delivery and Bone tissue engineering, as well as plasma display panel, Image Processing and cancer therapy applications etc.

ACKNOWLEDGEMENT

We gratefully acknowledge the kind support for the facility of XRD analysis Dept. of Metallurgical Engineering and FTIR analysis Dept. of physics, NIT Raipur (C.G.). Authors are also thankful to Dept. of physics, Pt. Ravishankar Shukla University, Raipur (C.G.) for providing us the facility of Photoluminescence analysis. We are also heartily grateful to Dept. of physics, Dr. Radha Bai, Govt. Navin Girls College Mathpara Raipur (C.G.), providing the facility of muffle furnace and other essential research equipments.

COMPETING INTERESTS

Authors have declared that no competing interests exist.

REFERENCES

1. Schubert EF, Kim JK. Solid-state light sources getting smart. Science. 2005;308(5726):1274-8.
2. Feldmann C, Jüstel T, Ronda CR, Schmidt PJ. Inorganic luminescent materials: 100 years of research and application. Advanced Functional Materials. 2003;13(7):511-6.
3. Jüstel T, Nikol H, Ronda C. New developments in the field of luminescent materials for lighting and displays. Angewandte Chemie International Edition. 1998;37(22):3084-103.
4. Chen TM, Chen SC, Yu CJ. Preparation and characterization of garnet phosphor nanoparticles derived from oxalate coprecipitation. Journal of solid state chemistry. 1999;144(2):437-441.
5. Jung KY, Lee HW, Kang YC, Park SB, Yang YS. Luminescent properties of (Ba, Sr) $MgAl_{10}O_{17}$: Mn, Eu green phosphor prepared by spray pyrolysis under VUV excitation. Chemistry of materials. 2005;17(10):2729-2734.
6. Chakradhar RS, Nagabhushana BM, Chandrappa GT, Ramesh KP, Rao JL. Solution combustion derived nanocrystalline macroporouswollastonite ceramics. Materials Chemistry and Physics. 2006;95(1):169-175.
7. Bhatkar VB, Bhatkar NV. Combustion synthesis and photoluminescence study of silicate biomaterials. Bulletin of Materials Science. 2011;34(6):1281-1284.
8. Verma BR, Baghel RN, Bisen DP, Brahme N, Khare A. Luminescent characterization of $CaMgSiO_4$: Dy^{3+} phosphor for white light emitting diodes. In IOP Conference Series: Materials Science and Engineering. IOP Publishing. 2020;798(1):012009).
9. Shukla D, Ghormare KB, Dhoble SJ. Wet chemical synthesis and photoluminescence characteristics of $Ca_5(PO_4)_3F$: Dy phosphor. Adv. Mat. Lett. 2014;5(7):406-408.
10. Poort SHM, Janssen, W., &Blasse, G. Optical properties of Eu^{2+}-activated

orthosilicates and orthophosphates. Journal of Alloys and Compounds. 1997;260(1-2):93-97.
11. Pandey D, Brahme DR, Sharma DN. Study of Optical Properties of Di Calcium-Magnesium Di Silicate Based Phosphors Dysprosium Doped Rare Earth Material. International Journal of Advanced Research. 2016;4(1):1639-1646.
12. Pandey D, Brahme DN, Sharma DR. Thermo-Luminescence Properties of Ce^{3+} & Dy^{3+} Doped Di Calcium Magnesium Di Silicate, $Ca_2MgSi_2O_7$.
13. Jiang L, Chang C, Mao D, Feng C. Luminescent properties of $Ca_2MgSi_2O_7$ phosphor activated by Eu^{2+}, Dy^{3+} and Nd^{3+}. Optical Materials. 2004;1,27(1):51-5.
14. Vinicius Ribas De Morais, Preparation Of Dy^{3+} Doped Calcium Magnesium Silicate Phosphors by a New Synthesis Method and Its Luminescence Characterization. In the Proceedings of the 2018, 7th International Congress On Ceramics & 62nd Congress Brasileiro De Ceramica, Foz Do Iguacu- Pr Brazil June 2018;17-21.
15. Raut SK, Dhoble NS, Dhoble SJ. Journal of search & research. 2011;2(2):36-39.
16. Kingsley JJ, Patil KC. A novel combustion process for the synthesis of fine particle α-alumina and related oxide materials. Materials letters. 1988,1,6(11-12):427-32.
17. JCPDS PDF File No. 17-1149, JCPDS International Center for Diffraction Data.
18. Data-Base-Code AMCSD 0008032.
19. Feitosa AV, Miranda MAR, Sasaki JM, Arujo-Silva MA. Braz.J.Phys. 2004;34 (2B):656
20. Ubale AU, Sangawar VS, Kulkarni DK. Size dependent optical characteristics of chemically deposited nanostructured ZnS thin films. Bulletin of Materials Science. 2007;1,30(2):147-51.
21. Shannon RD. Revised effective ionic radii and systematic studies of interatomic distances in halides and chalcogenides. Acta crystallographica section A: crystal physics, diffraction, theoretical and general crystallography. 1976;32(5):751-67.
22. Qin Fei C, Chang D, Mao J. Alloy. Compd., 2005;390(1-2):134-137.
23. Frost RL, Bouzaid JM, Reddy BJ. Vibrational spectroscopy of the sorosilicate mineral hemimorphite $Zn_4(OH)_2Si_2O_7·H_2O$. Polyhedron. 2007;26(12):2405-12.
24. Chandrappa GT, Ghosh S, Patil KC. Synthesis and Properties of Willemite, Zn_2SiO_4, and M^{2+}:Zn_2SiO_4 (M= Co and Ni). Journal of Materials Synthesis and Processing. 1999;7(5):273-9.
25. Makreski G, Jovanovski B, Kaitner A, Gajovic T. Biljan, Vib. Spectrosc., 2007;44:162.
26. Caracas R, Gonze X. Ab initio determination of the ground-state properties of $Ca_2MgSi_2O_7$ åkermanite. Physical Review B. 2003;68(18):184102.
27. Salim MA, Hussain R, Abdullah MS, Abdullah NS, Alias SA, Ahmad Fuzi MN, Md Yusuf KM. Mahbor, Solid State Sci. Technol. 2009; 17(2):59–64.
28. Lin L, Yin M, Shi C, Zhang W. Journal of Alloys and Compounds. 2008;455(1-2):327-330.
29. Zhu L, Zuo C, Luo Z, Lu A. Photoluminescence of Dy^{3+} and Sm^{3+}: SiO_2–Al_2O_3–LiF–CaF_2 glasses. Physica B: Condensed Matter. 2010;405(21):4401-6.
30. Chen Y, Cheng X, Liu M, Qi Z, Shi C. Comparison study of the luminescent properties of the white-light long afterglow phosphors: $Ca_xMgSi_2O_{5+x}$: Dy^{3+} (x= 1, 2, 3). Journal of luminescence. 2009;29(5):531-5.
31. Tshabalala MA, Dejene FB, Pitale SS, Swart HC, Ntwaeaborwa OM. Generation of White-Light from Dy^{3+} Doped Sr_2SiO_4 Phosphor Phys. 2014:126-129.
32. Vishwakarma AK, Jha K, Jayasimhadri M, Sivaiah B, Gahtori B, Haranath D. US National libraray of medicine, National institute of health, (pub. Med.gov.). 2015; 44(39):17166-74.

© 2021 Sharma et al.; This is an Open Access article distributed under the terms of the Creative Commons Attribution License (http://creativecommons.org/licenses/by/4.0), which permits unrestricted use, distribution, and reproduction in any medium, provided the original work is properly cited.

Peer-review history:
The peer review history for this paper can be accessed here:
https://www.sdiarticle4.com/review-history/77178